Article

Autoxidation of 4-Hydrazinylquinolin-2(1*H*)-one; Synthesis of Pyridazino[4,3-*c*:5,6-*c'*]diquinoline-6,7(5*H*,8*H*)-diones

Sara M. Mostafa [1], Ashraf A. Aly [1,*], Alaa A. Hassan [1], Esraa M. Osman [1], Stefan Bräse [2,3,*], Martin Nieger [4], Mahmoud A. A. Ibrahim [1] and Asmaa H. Mohamed [1]

[1] Chemistry Department, Faculty of Science, Minia University, El Minia 61519, Egypt;
sara.ahmed@mu.edu.eg (S.M.M.); alaahassan2001@mu.edu.eg (A.A.H.); esraamah33@gmail.com (E.M.O.);
m.ibrahim@compchem.net (M.A.A.I.); asmaa.hamouda@mu.edu.eg (A.H.M.)

[2] Institute of Organic Chemistry, Karlsruhe Institute of Technology, Eggenstein-Leopoldshafen,
76131 Karlsruhe, Germany

[3] Institute of Biological and Chemical Systems (IBCS-FMS), Karlsruhe Institute of Technology,
Eggenstein-Leopoldshafen, 76131 Karlsruhe, Germany

[4] Department of Chemistry, University of Helsinki, P.O. Box 55 (A. I. Virtasen aukio I), 00014 Helsinki, Finland;
martin.nieger@helsinki.fi

* Correspondence: ashraf.shehata@mu.edu.eg (A.A.A.); stefan.braese@kit.edu.eg (S.B.)

Abstract: An efficient synthesis of a series of pyridazino[4,3-*c*:5,6-*c'*]diquinolines was achieved via the autoxidation of 4-hydrazinylquinolin-2(1*H*)-ones. IR, NMR (^{1}H and ^{13}C), mass spectral data, and elemental analysis were used to fit and elucidate the structures of the newly synthesized compounds. X-ray structure analysis and theoretical calculations unequivocally proved the formation of the structure. The possible mechanism for the reaction is also discussed.

Keywords: 4-hydrazinylquinolin-2(1*H*)-one; pyridazino[4,3-*c*:5,6-*c'*]diquinoline-6,7(5*H*,8*H*)-dione; autoxidation reaction; X-ray; DFT

1. Introduction

Compounds with quinolin-2(1*H*)-one (carbostyril) skeletons are present in a large number of biologically active compounds [1–12]. During the twentieth century [13], various research groups dealt with the chemistry and biological applications of quinolines [14].

Pyridazine and its polycyclic structures have still played an interesting role in organic chemistry because of their remarkable properties in forming supramolecular assembly [15–18]. Pyridazine molecules are important heterocycle scaffolds that reveal diverse biological activities in medicine [19–25] and agriculture [26]. For example, Pyridazomycin is an antifungal and antibiotic compound, the first pyridazine derivative isolated from a natural source [27]. In contrast, Pyridaben is widely used as an acaricide with a long residual action, whereas Chloridazone has a long history of use as an herbicide [28]. Minaprine is a psychotropic drug that has effectively treated various depressive states [29] (Figure 1).

Functionalized pyridazines have high electron-deficient properties, encouraging their utilization as electrochromic materials and metal–organic frameworks [30,31].

Hydrazines have shown basic and reducing characteristics that enable their utility in many industrial and medical applications. Accordingly, hydrazines have served as rocket fuel, antioxidants, oxygen scavengers, and as intermediates for the production of explosives, propellants, and pesticides [32].

It has been demonstrated that oxygen makes hydrazine solutions unstable, especially under alkaline or neutral conditions. However, hydrazines are stable under strongly acidic conditions or without oxygen [33].

Wagnerova et al. [34] have reported that cobalt-tetrasulphophthalocyanines enhance the autoxidation process of hydrazines [34]. On the other hand, Ichiro Okura et al. [35] reported that the autoxidation of hydrazine occurred with manganese (III)-hematoporphyrin

at room temperature, and that has an advantage because of its reactivity for the formation of oxygen coordinated Mn(III)-Hm peroxide adduct [36]. Andrew P. Hong et al. [37] reported that satisfactory autoxidation of hydrazines occurred using cobalt (II) 4,4′,4″,4‴-tetrasulfophthalocyanine (CoIITSP).
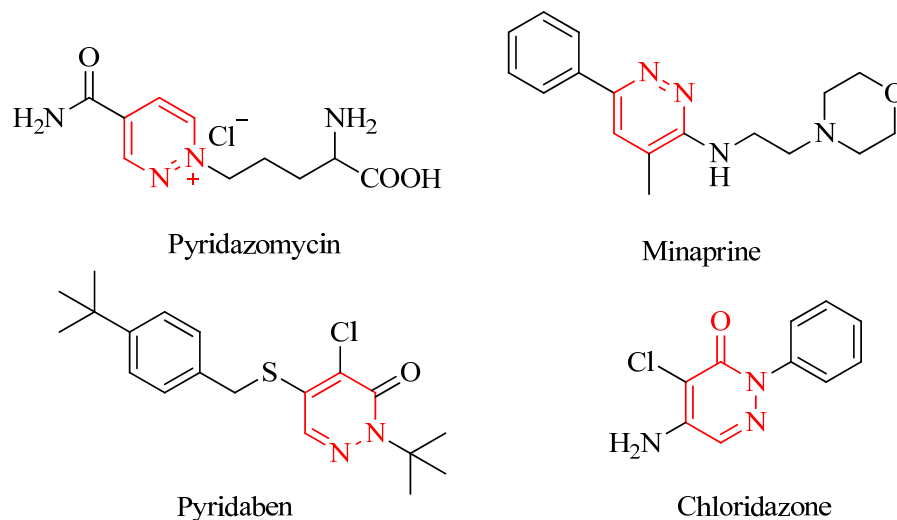

Figure 1. Chemical structures of biologically active Pyridazomycin, Minaprine, Pyridaben and Chloridazone.

Previously, it was reported [38] that 1-ethyl-4-hydroxyquinolin-2(1*H*)-one (**1**) reacted with hydrazine hydrate, in 1,2-dichlorobenzene (*o*-DCB), to give a mixture of two compounds. These compounds were separated using fractional recrystallization to give quinolinylhydrazine **2a** in 19% yield and diquinopyridazine **3a** in 41% yield (Scheme 1).
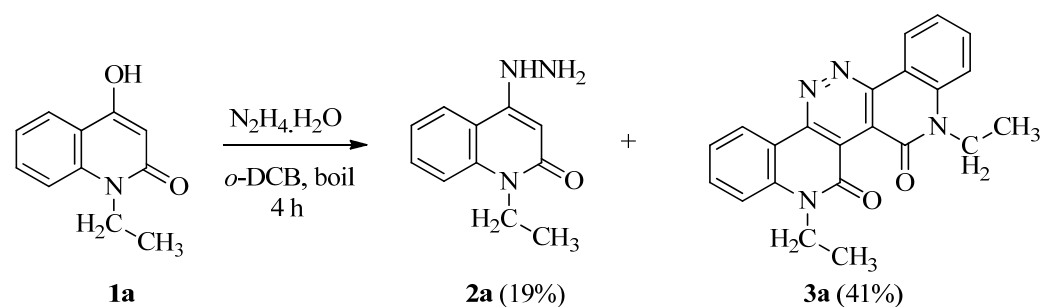
Scheme 1. Formation of compound **3a** from the reaction of 1-ethyl-4-hydroxyquinolin-2(1*H*)-one (**1**) with hydrazine in *o*-DCB.

A convenient microwave-assisted, one-pot, four-component synthetic approach was developed as a route to functionalized benzo[a]pyridazino[3,4-c]phenazine derivatives starting from 2-hydroxy-1,4-naphthoquinone, aromatic aldehydes, methyl hydrazine, and *o*-phenylenediamine. Compounds of a similar pentacyclic structure such as bisanthranilate showed an intramolecular electrophilic cyclization and afforded an angular *cis*-quinacridone compound, which condensed with hydrazine to give a phthalazine derivative [39]. The biological profiles of some of the compounds mentioned above exhibited good cytotoxic activities against KB, HepG2, Lu1, and MCF7 human cancer cell lines. In addition, a compound of the derivatives exhibited promising antimicrobial activities toward *Staphylococcus aureus* and *Bacillus subtilis* bacterial strains with IC$_{50}$ < 6 μM [40].
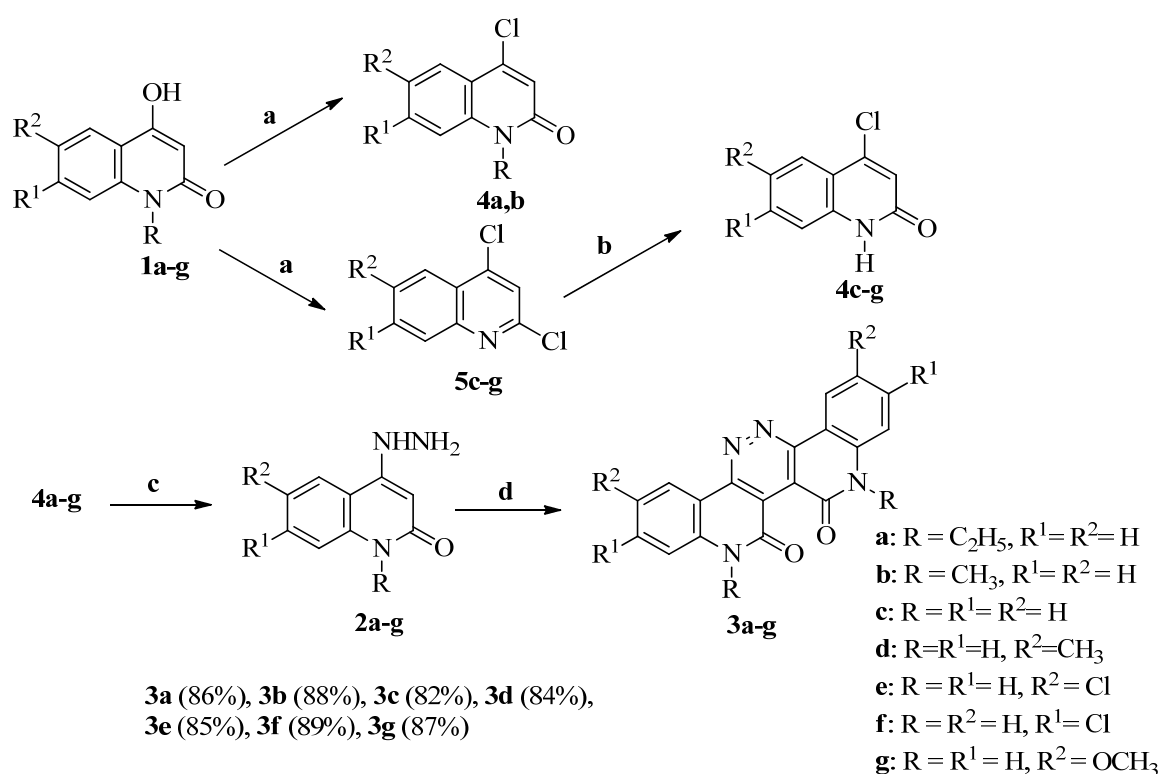
Recently, it has been reported that hydrazines can be used as catalysts for removing oxygen in the closing carbonyl–olefin metathesis process [41]. We have also found that prolongated reflux during the formylation process of 2-quinolones *via* a DMF/Et$_3$N mixture caused

dimerization to occur, and unexpected 3,3′-methylenebis(4-hydroxyquinolin-2(1*H*)-ones) were obtained [42].

The above-mentioned findings encouraged us to generalize the method of preparation for heteroannulated pentacyclic compounds with the structure of this interesting molecule.

2. Results and Discussion

The strategy started with the preparation of derivatives of compounds **1**, **2**, **4**, and **5** according to reported methods, and their structures were confirmed by matching their spectral data with those reported [43–45]. The key intermediates, hydrazine quinolones **2a–g**, were prepared by refluxing compounds **4a–g** with hydrazine hydrate (Scheme 2) [46]. During the heating of 4-hydrazinylquinolin-2(1*H*)-ones **2a–g** in pyridine, we observed the abnormal formation, in good yields, of pyridazino[4,3-*c*:5,6-*c*′]diquinoline-6,7- (5*H*,8*H*)-diones **3a–g**. As had been suggested, compounds **2a–g** underwent an autoxidation reaction.

3a (86%), **3b** (88%), **3c** (82%), **3d** (84%),
3e (85%), **3f** (89%), **3g** (87%)

a: R = C$_2$H$_5$, R^1= R^2= H
b: R = CH$_3$, R^1= R^2 = H
c: R = R^1= R^2= H
d: R=R^1=H, R^2=CH$_3$
e: R = R^1= H, R^2 = Cl
f: R = R^2= H, R^1= Cl
g: R = R^1 = H, R^2 = OCH$_3$

Scheme 2. Synthesis of pyridazino[4,3-*c*:5,6-*c*′]diquinoline-6,7(5*H*,8*H*)-diones **3a–g**. Reagents and conditions: (a) POCl$_3$, reflux, 2 h; (b) AcOH, reflux 12 h; (c) NH$_2$.NH$_2$.H$_2$O, reflux 12 h; (d) pyridine reflux, 6–12 h.

The structures of the products **3a–g** were proved from their elemental analyses and IR, ^{1}H NMR, and ^{13}C NMR spectra. For example, the mass spectrum and elemental analysis of **3a** established its molecular formula as C$_{22}$H$_{18}$N$_4$O$_2$. The ^{1}H NMR spectrum of **3a** exhibited the ethyl protons as a triplet at δ_H = 1.22 (*J* = 7.6 Hz) for CH$_3$ and a quartet at δ_H = 4.39 ppm (*J* = 7.6 Hz) for CH$_2$. The eight aromatic protons appeared as three multiplets at δ_H = 7.36–7.40 for 2H, 7.68–7.78 for 4H, and 8.06–8.08 ppm for 2H. The reported spectroscopic data for the ^{13}C NMR spectrum of compound **3a** showed the carbonyl-quinolone, 2NCH$_2$, and CH$_3$ carbon signals at δ_C = 165.72, 39.11, and 14.11 ppm, respectively. Similar spectroscopic results of compound **3a** were also reported [38]. The structure of **3a** was unambiguously determined by a single crystal structure (Figure 2).
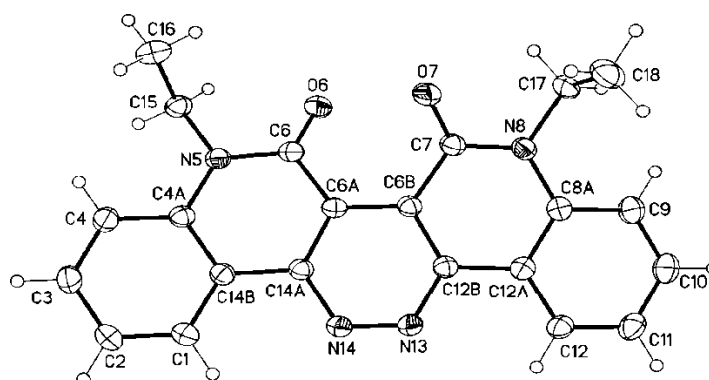
Figure 2. Molecular structure of one of the crystallographic independent molecules of **3a**.

We carried out the reaction in different conditions using compound **1a** as an example with the optimized reaction conditions. In EtONa/EtOH (Method **B**, Table 1), it was found that the yield of **3a** was decreased (74%). Refluxing of **1a** in toluene/Et$_3$N (Method **C**, Table 1) did not increase the yield (60%), and the time taken to obtain **3a** was increased (2d). Furthermore, adding a few drops of Et$_3$N to DMF (Method **D**, Table 1) improved the yield of **3a** compared with methods **B** and **C**, but it was still lower compared with our method **A**. Using Na/toluene, the oxidation of **1a** occurred satisfactorily; however, it was lower compared with method **A**. In our trial of an acidic medium using HCl/EtOH mixture, the reaction failed. Thus, the best condition to obtain high yields and a short reaction time of **3a–g** is reflux in dry pyridine (Method **A**, Table 1).

Table 1. The reaction optimization for the formation of **3a**.

Entry	Method	Yields of 3a (%)
A	Pyridine, reflux, 8 h	88
B	EtONa/EtOH, reflux 24 h [a]	74
C	Toluene/Et$_3$N, reflux, 2 d [b]	60
D	DMF/Et$_3$N, reflux 20 h [c]	78
E	Na/Toluene, reflux 18 h [d]	82
F	EtOH/HCl, reflux [e]	No reaction

[a] 1 mmol of **2a** and 0.1 mmol of EtONa in 100 mL of absolute EtOH at 70 °C. [b] 1 mmol of **2a** + 0.5 mL of Et$_3$N in 30 mL of toluene at 80 °C. [c] 1 mmol of **2a** + 0.5 mL of Et$_3$N in 15 mL of DMF at 100 °C. [d] 1 mmol of **2a** + 0.5 mol of Na in 30 mL of toluene at 80 °C. [e] 1 mmol of **2a** + 1 mL of 0.1 M HCl in 100 mL of absolute EtOH at 70 °C.

The formation of pyridazino[4,3-c:5,6-c']diquinoline-6,7(5*H*,8*H*)-diones **3a–g** can be rationalized as depicted in Scheme 3. It is clear from the suggested mechanism (Scheme 3) that it constitutes several steps of nucleophilic substitution, dimerization, autoxidation, and electrocyclic reactions in a one-pot process leading to the pentacyclic final products **3a–g**. The mechanism starts with a proton shift of compound **2** to its isomer **2′** (Scheme 3). Then, the starting molecule of **2** reacts with its isomer **2′** to give **6** (Scheme 3). The elimination of a hydrazine molecule in **6** would give the dimerized hydrazone **7**, which undergoes another proton shift to give the intermediate **7′**. Because the reaction did not proceed under an inert argon atmosphere (i.e., under argon atmosphere, the starting quinolinyl-hydrazines **2a–g** were recovered), we proposed that the intermediate **7′** undergo an aerial oxidation NH-NH group to give the intermediate **8**. After that, the intermediate **8** would undergo internal electrocyclization to give **9**. Finally, another mode of aerial oxidation of **9** would produce compound **3** (Scheme 3).
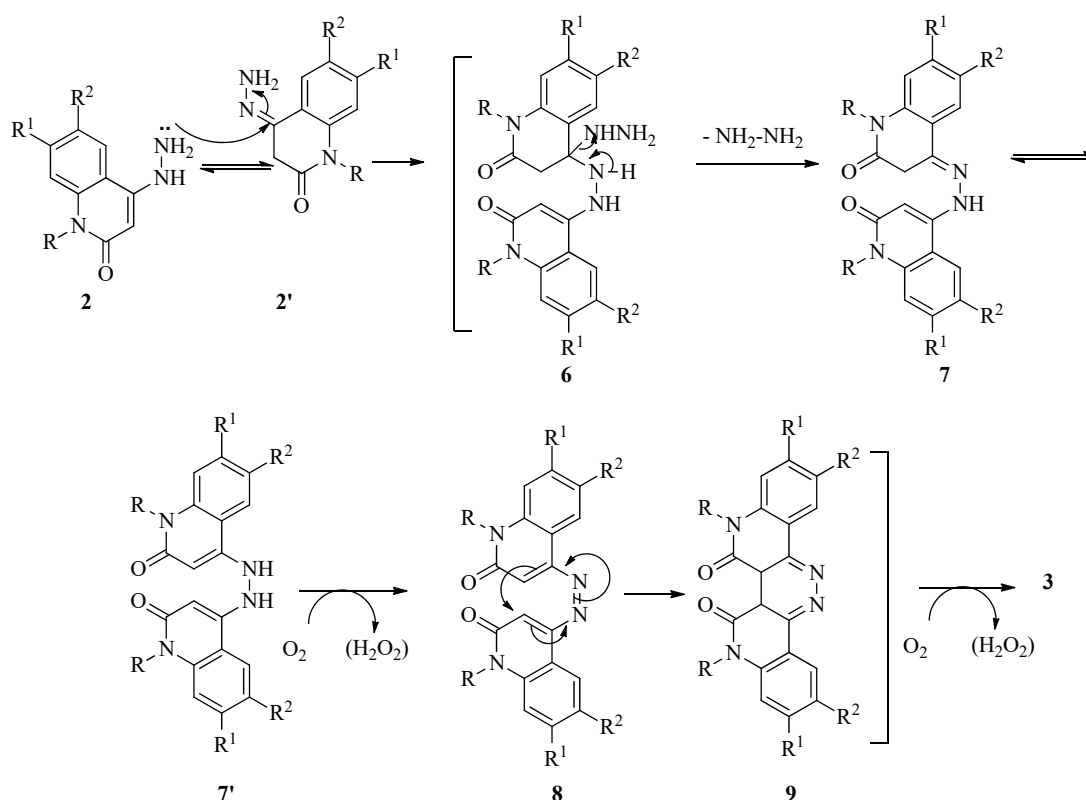
Scheme 3. The suggested mechanism describes the formation of compounds **3a–g**.

The preceding literature supports the mechanism [47] describing aryl hydrazine chlorides' aerial oxidation into diazines. Accordingly, it supports the steps of transformations of **7′** into **8** and **9** into **3**. Moreover, aerial catalytic oxidation in pyridine transformed hydrazones into diazo compounds [48].

Firstly, the stability of compound **3a** (Figure 3), as an example, was described. Therefore, the quantum mechanical calculations were performed for compound **3a**. The investigated compound was first optimized using the DFT method (see the Methods section for details). The optimized structure was then subjected to vibrational frequency and single-point energy calculations. The quantum theory of atoms in molecules (QTAIM) was invoked to achieve an in-depth insight into the topological features of compound **3a** [49]. In the context of QTAIM, the (3,–1) bond critical points (BCPs) and bond paths (BPs) were generated, and the electron density was computed. Moreover, noncovalent interaction (NCI) index analysis was executed to pictorially elucidate the origin and nature of intramolecular interactions within compound **3a** [50]. According to the results, no imaginary frequencies were observed for the investigated structure of compound **3a**, confirming that this conformer is a true minimum. Based on the QTAIM results presented in Figure 4a, the occurrence of intramolecular bonds within the inspected compound was revealed by the existence of BPs and BCPs. Chalcogen⋯chalcogen intramolecular interaction was also noticed in compound **3a** via the BP and BCP between the two oxygen atoms (O⋯O). The BCP at the BP O⋯O within compound **3a** exhibited electron density with a value of 0.0144 au.

The stability of compound **3a** might also be interpreted as a consequence of the aromatic planarity, which could be detected from Figure 4a *via* dihedral angles (Φ) with a value of 1.83°. Notably, the difference between the dihedral angle of the optimized geometry of compound **3a** and the X-ray data was nearly 0.36°.

As shown in Figure 4b, the NCI results (green isosurfaces) occurred at the interatomic space between the interacting atoms, asserting the occurrence of the intramolecular interactions towards the investigated compound. Large, green, round domains within the

intramolecular forces $N_{13} \cdots HC_{12}$ and $N_{14} \cdots HC_1$ of compound **3a** were crucially denoted, reflecting the favorable contribution of such intramolecular forces to the further stability of compound **3a**.
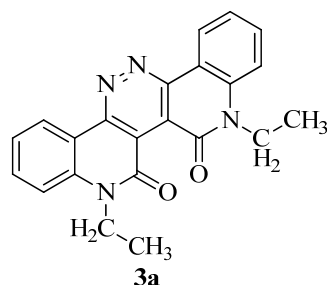

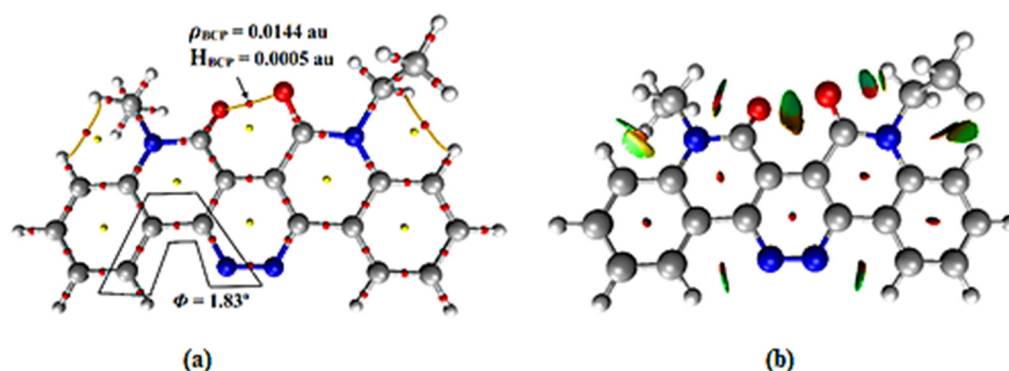**Figure 3.** The assigned structure of compound **3a**.

Figure 4. (**a**) Quantum theory of atoms in molecules (QTAIM) and (**b**) 3D noncovalent interaction (NCI) isosurfaces for compound **3a**. The isosurfaces were generated with a reduced density gradient value of 0.50 au and colored from blue to red according to sign (λ_2), ρ ranging from −0.035 (blue) to 0.020 (red) au.

3. Conclusions

The unprecedented dimerization and oxidation cascade of 4-hydrazinylquinolin-2(1*H*)-ones delivered pyridazino[4,3-*c*:5,6-*c′*]diquinoline-6,7(5*H*,8*H*)-diones in good yields. The synthesis of the obtained pyridazino-diquinolones was achieved in different conditions. Heating 4-hydrazinylquinolin-2(1*H*)-ones in pyridine was the best condition in which to obtain the corresponding products. Quantum mechanical calculations were also performed using the DFT method to prove the stability of the formed products. The method above can be used as a general method for the preparation of various classes of pentacyclic heterocycles from compounds with structural features similar to 4-hydroxy-2-quinolones. Importantly, the biological activity of the obtained products could assist in the development of new drugs.

4. Experimental Section

4.1. Chemistry

The IR spectra were recorded using the ATR technique (ATR = Attenuated Total Reflection) with an FT device (FT-IR Bruker IFS 88), Institute of Organic Chemistry, Karlsruhe University, Karlsruhe, Germany. The NMR spectra were measured in DMSO-d_6 on a Bruker AV-400 spectrometer, 400 MHz for ^{1}H, and 100 MHz for ^{13}C; the chemical shifts are expressed in δ (ppm), versus internal tetramethylsilane (TMS) = 0 for ^{1}H and ^{13}C, and external liquid ammonia = 0. The description of signals includes: s = singlet, d = doublet, t = triplet, q = quartet, m = multiplet, dd = doublet of doublet, and m = multiplet. Mass spectra were recorded on a FAB (fast atom bombardment) Thermo Finnigan Mat 95 (70 eV). Elemental analyses were carried out at the Microanalytical Center, Cairo University, Egypt.

TLC was performed on analytical Merck 9385 silica aluminum sheets (Kieselgel 60) with Pf254 indicator; TLCs were viewed at λmax = 254 nm.

4.1.1. Starting Materials

4-Chloro-quinolin-2(1*H*)-ones **4a–g** were prepared according to the literature [43–45], whereas 4-hydrazinylquinolin-2(1*H*)-ones **2a–g** were synthesized according to the literature [46].

4.1.2. General Procedure

4-Hydrazinylquinolin-2(1*H*)-ones **2a–g** (1 mmol) were heated in pyridine for 6–12 h until the reactants had disappeared, as mentioned in Scheme 1. The reaction was monitored using TLC (using toluene: EtOAc; 10:1). Then, the mixture was cooled and poured into iced water; the formed precipitate was filtered, washed with water, and recrystallized from the stated solvents to give pure crystals **3a–g**.

5,8-Diethylpyridazino[4,3-*c*:5,6-*c'*]diquinoline-6,7(5*H*,8*H*)-dione (**3a**)

Orange crystals (DMF/H_2O), yield: 0.31 g (86%); mp 330–332 °C. IR (KBr): υ = 3013 (Ar-CH), 2927 (Ali-CH), 1653 (C=O), 1603, 1561 (Ar-C=C) cm^{-1}; NMR as reported in ref. [38].

5,8-Dimethylpyridazino[4,3-*c*:5,6-*c'*]diquinoline-6,7(5*H*,8*H*)-dione (**3b**)

Orange crystals (DMF/EtOH), yield: 0.30 g (88%); mp 320–322 °C. IR (KBr) υ = 3023 (Ar-CH), 2929 (Ali-CH), 1652 (C=O), 1604, 1586 (Ar-C=C) cm^{-1}; ^{1}H NMR (400 MHz, DMSO-d_6) δ_H = 3.72 (s, 6H, CH$_3$), 7.38–7.40 (m, 2H, Ar-H), 7.71–7.76 (m, 4H, Ar-H), 8.03–8.06 (m, 2H, Ar-H); ^{13}C NMR (100 MHz, DMSO-d_6): δ_C = 39.91 (2 CH$_3$), 115.87, 115.78, 119.12, 122.14, 122.25, 131.66, 136.82, 156.61, 165.81 ppm (C-6 and C-7); MS (Fab, 70 eV, %): *m/z* = 342 (M$^+$, 82), 289 (6), 197 (13), 171 (23), 169 (36), 157 (100), 134 (48), 105 (15). *Anal. Calcd. for* C$_{20}$H$_{14}$N$_4$O$_2$ (342.35): C, 70.17; H, 4.12; N, 16.37. Found: C, 70.09; H, 4.23; N, 16.44.

Pyridazino[4,3-*c*:5,6-*c'*]diquinoline-6,7(5*H*,8*H*)-dione (**3c**)

Orange crystals (DMF/H_2O), yield: 0.257 g (82%); mp 348–350 °C. IR (KBr) υ =3174 (NH), 3044 (Ar-CH), 1640 (C=O), 1602, 1585 (Ar-C=C) cm^{-1}; ^{1}H NMR (400 MHz, DMSO-d_6) δ_H = 7.05–7.09 (m, 2H, Ar-H), 7.18–7.23 (m, 2H, Ar-H), 7.33–7.38 (m, 2H, Ar-H), 7.68 (dd, 2H, *J* = 7.8, 1.2 Hz, Ar-H), 11.99 (s, 2H, NH); ^{13}C NMR (100 MHz, DMSO-d_6): δ_C = 115.85, 115.96, 119.12, 122.52, 122.78, 130.87, 136.80, 157.77, 165.94 ppm (C-6 and C-7); MS (Fab, 70 eV, %): *m/z* = 314 (M$^+$, 15), 287 (45), 243 (6), 228 (70), 171 (12), 157 (84). *Anal. Calcd. for* C$_{18}$H$_{10}$N$_4$O$_2$ (314.30): C, 68.79; H, 3.21; N, 17.83. Found: C, 68.68; H, 3.35; N, 17.77.

2,11-Dimethylpyridazino[4,3-*c*:5,6-*c'*]diquinoline-6,7(5*H*,8*H*)-dione (**3d**)

Orange crystals (DMF/H_2O), yield: 0.287 g (84%); mp 352–354 °C. IR (KBr) υ = 3178 (NH), 3052 (Ar-CH), 1643 (C=O), 1606, 1581 (Ar-C=C) cm^{-1}; ^{1}H NMR (400 MHz, DMSO-d_6) δ_H = 2.37 (s, 6H, CH$_3$), 7.20–7.29 (m, 2H, Ar-H), 7.30–7.40 (m, 2H, Ar-H), 7.70 (d, 2H, *J* = 1.7 Hz, Ar-H), 12.21 (s, 2H, NH); ^{13}C NMR (100 MHz, DMSO-d_6): δ_C = 20.59 (2 CH$_3$), 115.77, 115.88, 119.12, 122.14, 131.66, 132.15, 134.82, 157.62, 165.71 ppm (C-6 and C-7); MS (Fab, 70 eV, %): *m/z* = 342 (M$^+$, 25), 327 (20), 312 (5), 271 (38), 171 (100), 157 (30). *Anal. Calcd. for* C$_{20}$H$_{14}$N$_4$O$_2$ (342.35): C, 70.17; H, 4.12; N, 16.37. Found: C, 70.25; H, 4.03; N, 16.25.

2,11-Dichloropyridazino[4,3-*c*:5,6-*c'*]diquinoline-6,7(5*H*,8*H*)-dione (**3e**)

Orange crystals (DMF/H_2O), yield: 0.325 g (85%); mp 358–360 °C. IR (KBr) υ = 3177 (NH), 3023 (Ar-CH), 1640 (C=O), 1605, 1560 (Ar-C=C) cm^{-1}; ^{1}H NMR (400 MHz, DMSO-d_6) δ_H = 7.34–7.35 (m, 2H, Ar-H), 7.36–7.37 (m, 2H, Ar-H), 7.68–7.70 (m, 2H, Ar-H), 12.19 (s, 2H, NH); ^{13}C NMR (100 MHz, DMSO-d_6): δ_C = 115.78, 115.92, 119.12, 122.10, 128.78, 132.87, 136.80, 157.52, 165.12 ppm (C-6 and C-7); MS (Fab, 70 eV, %): *m/z* = 383 (M$^+$, 100), 348 (9),

313 (49), 305 (6), 227 (37), 191 (14). *Anal. Calcd. for* $C_{18}H_8Cl_2N4O_2$ (383.19): C, 56.42; H, 2.10; N, 14.62. Found: C, 56.51; H, 2.17; N, 14.53.

3,10-Dichloropyridazino[4,3-*c*:5,6-*c′*]diquinoline-6,7(5*H*,8*H*)-dione (**3f**)

Orange crystals (DMF/EtOH), yield: 0.341 g (89%); mp 358–360 °C. IR (KBr) υ = 3180 (NH), 3041 (Ar-CH), 1645 (C=O), 1610, 1567 (Ar-C=C) cm^{-1}; ^{1}H NMR (400 MHz, DMSO-d_6) δ_H = 7.20–7.35 (m, 2H, Ar-H), 7.37–7.38 (m, 2H, Ar-H), 7.70 (d, 2H, *J* = 7.8 Hz, Ar-H), 12.20 (s, 2H, NH); ^{13}C NMR (100 MHz, DMSO-d_6): δ_C = 115.77, 115.88, 119.12, 122.14, 131.12, 132.15, 136.82, 157.62, 164.71 ppm (C-6 and C-7); MS (Fab, 70 eV, %): *m/z* = 383 (M$^+$, 70), 313 (31) 227 (14), 191 (100), 153 (89), 137 (31), 110 (18). *Anal. Calcd. for* $C_{18}H_8Cl_2N_4O_2$ (383.19): C, 56.42; H, 2.10; N, 14.62. Found: C, 56.30; H, 2.19; N, 14.55.

2,11-Dimethoxypyridazino[4,3-*c*:5,6-*c′*]diquinoline-6,7(5*H*,8*H*)-dione (**3g**)

Orange crystals (DMF/EtOH), yield: 0.325 g (87%); mp 354–356 °C. IR (KBr) υ = 3186 (NH), 3039 (Ar-CH), 1648 (C=O), 1607, 1577 (Ar-C=C) cm^{-1}; ^{1}H NMR (400 MHz, DMSO-d_6) δ_H = 3.82 (s, 6H, OCH$_3$), 7.20–7.23 (m, 2H, Ar-H), 7.32–7.33 (m, 2H, Ar-H), 7.34–7.37 (m, 2H, Ar-H), 12.13 (s, 2H, NH); ^{13}C NMR (100 MHz, DMSO-d_6): δ_C = 55.37 (2 OCH$_3$), 116.53, 117.54, 120.53, 122.52, 131.30, 132.80, 134.47, 157.77, 165.73 ppm (C-6 and C-7); MS (Fab, 70 eV, %): *m/z* = 374 (M$^+$, 100), 313 (36), 284 (55), 268 (46), 187 (50), 106 (18). *Anal. Calcd. for* $C_{20}H_{14}N_4O_4$ (374.35): C, 64.17; H, 3.77; N, 14.97. Found: C, 64.23; H, 3.60; N, 15.09.

4.1.3. Crystal Structure Determination

Single crystals were obtained via recrystallization from DMF/Water. The single-crystal X-ray diffraction study of **3a** was carried out on a Bruker D8 VENTURE diffractometer with a PhotonII CPAD detector at 298 K using Cu-Kα radiation (λ = 1.54178 Å). Dual space methods (SHELXT) [51] were used for structure solution, and refinement was carried out using SHELXL [51] (full-matrix least-squares on F^2). Hydrogen atoms were localized using difference electron density determination and refined using a riding model (H(N) free). A semi-empirical absorption correction was applied. The absolute structure was determined via the refinement of Parsons' x-parameters [52].

3a: Orange crystals: $C_{22}H_{18}N_4O_2$, M$_r$ = 370.40 g mol^{-1}, size 0.20 × 0.12 × 0.04 mm, Orthorhombic, Pca2$_1$ (no.29), *a* = 21.1937 (4) Å, *b* = 9.2208 (2) Å, *c* = 17.9646 (3) Å, *V* = 3510.69 (12) Å^3, Z = 8, D$_{calcd}$ = 1.402 Mg m^{-3}, F(000) = 1552, μ (Cu-Kα = 0.75 mm^{-1}, *T* = 298 K, 36,156 measured reflection (2θ$_{max}$ = 144.40), 6865 independent (R$_{int}$ = 0.057), 506 parameters, 1 restraint, R$_1$ (for 6684 *I* > 2σ(1)) = 0.042, *wR*^{2} (for all data) = 0.115, *S* = 1.02, largest diff. peak and hole = 0.34 eÅ^{-3}/−0.22 eÅ^{-3}, x = −0.05(11).

CCDC 2,128,843 (**3a**) contains the supplementary crystallographic data for this paper (see the Supplementary Materials). These data can be obtained free of charge from The Cambridge Crystallographic Data Centre via www.ccdc.cam.ac.uk/data_request/cif (accessed on 10 February 2022).

4.1.4. Theoretical Calculations

Geometrical optimization and vibrational frequency calculations were carried out at the B3LYP/6-31G* level of theory [53,54] for the compounds under consideration. Upon the optimized structures, the energetic features were then evaluated at MP2/6-311 + G** [55]//B3LYP/6-31G* levels of theory. QTAIM and NCI calculations were performed with the help of Multiwfn 3.7 package [56] and were plotted using Visual Molecular Dynamics (VMD) software [57]. All quantum mechanical calculations were carried out at the B3LYP/6-31G* level of theory using Gaussian 09 software (Gaussian, Inc.: Wallingford, CT, USA) [58].

References

1. Larghi, E.L.; Bruneau, A.; Sauvage, F.; Alami, M.; Vergnaud-Gauduchon, J.; Messaoudi, S. Synthesis and Biological Activity of 3-(Heteroaryl)quinolin-2(1*H*)-ones Bis-Heterocycles as Potential Inhibitors of the Protein Folding Machinery Hsp90. *Molecules* **2022**, *27*, 412. [CrossRef] [PubMed]
2. Shruthi, T.G.; Subramanian, S.; Eswaran, S. Design, Synthesis and Study of Antibacterial and Antitubercular Activity of Quinoline Hydrazone Hybrids. *Heterocycl. Commun.* **2020**, *26*, 137–147.
3. Elenich, O.V.; Lytvyn, R.Z.; Blinder, O.V.; Skripskaya, O.V.; Lyavinets, O.S.; Pitkovych, K.E. Synthesis and Antimicrobial Activity of 3-Phenyl-1-Methylquinolin-2-One Derivatives. *Pharmaceut. Chem. J.* **2019**, *52*, 969–974. [CrossRef]
4. Sharma, M.; Goyal, R.; Ahuja, D.; Sharma, A.; Soni, S.L. Antimicrobial and Antifungal Activity of Newly Synthesized 4-Hydroxy Quinoline Derivatives. *Eur. J. Mol. Clin. Med.* **2020**, *7*, 2082–2094.
5. Diaz, J.; Rodenas, D.; Ballester, F.J.; Alajarin, M.; Orenes, R.A.; Sanchez-Andrada, P.; Vidal, A. Unlocking the synthetic potential of aziridine and cyclopropane-fused quinolin-2-ones by regioselective fragmentation of its three-membered rings. *Arab. J. Chem.* **2020**, *13*, 2702–2714. [CrossRef]
6. Aly, A.A.; Ramadan, M.; Abuo-Rahma, G.E.A.; Elshaier, Y.A.M.M.; Elbastawesy, M.A.I.; Brown, A.B.; Bräse, S. Chapter Three—Quinolones as prospective drugs: Their syntheses and biological applications. *Adv. Heterocycl. Chem.* **2021**, *135*, 147–196.
7. Scavone, C.; Mascolo, A.; Ruggiero, R.; Sportiello, L.; Rafaniello, C.; Berrino, L.; Capuano, A. Quinolones-Induced Musculoskeletal, Neurological, and Psychiatric ADRs: A Pharmacovigilance Study Based on Data From the Italian Spontaneous Reporting System. *Front. Pharmacol.* **2020**, *11*, 428. [CrossRef]
8. Khamkhenshorngphanuch, T.; Kulkraisri, K.; Janjamratsaeng, A.; Plabutong, N.; Thammahong, A.; Manadee, K.; Pombejra, S.N.; Khotavivattana, T. Synthesis and Antimicrobial Activity of Novel 4-Hydroxy-2-quinolone Analogs. *Molecules* **2020**, *25*, 3059. [CrossRef]
9. Hassan, M.M.; Hassanin, H.M. An Efficient New Route for the Synthesis of Some 3-Hterocyclylquinolinones via Novel 3-(1,2-Dihydro-4-hydroxy-1-methyl-2-oxoquinolin-3-yl)-3-oxopropanal and Their Antioxidant Screening. *J. Heterocycl. Chem.* **2017**, *54*, 3321–3330. [CrossRef]
10. Wenjie, X.; Xueyao, L.; Guixing, M.; Hongmin, Z.; Ya, C.; Johannes, K.; Jie, X.; Song, W. N-thiadiazole-4-hydroxy-2-quinolone-3-carboxamides bearing heteroaromatic rings as novel antibacterial agents: Design, synthesis, biological evaluation and target identification. *Eur. J. Med. Chem.* **2020**, *188*, 112022.
11. Tzeng, C.C.; Lee, K.H.; Wang, T.C.; Han, C.H.; Chen, Y.L. Synthesis and Cytotoxic evaluation of a series of γ-substituted γ-aryloxymethyl-α-methylene-γ-butyrolactones against cancer cells. *Pharmaceut. Res.* **2000**, *17*, 715–719. [CrossRef] [PubMed]
12. Prajapati, S.M.; Patel, K.D.; Vekariya, R.H.; Panchal, S.N.; Patel, H.D. Recent advances in the synthesis of quinolines: A review. *RSC Adv.* **2014**, *4*, 24463–24476. [CrossRef]
13. Navneetha, O.; Deepthi, K.; Rao, A.M.; Jyostna, T.S. A review on chemotherapeutic activities of quinoline. *Int. J. Pharm. Chem. Biol. Sci.* **2017**, *7*, 364–372.
14. Constable, E.C.; Housecroft, C.E.; Neuburger, M.; Reymann, S.; Schaffner, S. 4-Substituted and 4,5-disubstituted 3,6-di(2-pyridyl)pyridazines: Ligands for supramolecular assemblies. *Eur. J. Org. Chem.* **2008**, *9*, 1597–1607. [CrossRef]
15. Bodman, S.E.; Fitchett, C.M. Silver complexes of symmetrically 4,5-disubstituted 3,6-di(3,5-dimethyl-1*H*-pyrazol-1-yl)pyridazine. *Supramol. Chem.* **2015**, *27*, 840–846. [CrossRef]

16. Wu, X.; Ji, H. Rhodium-Catalyzed [4 + 1] Cyclization via C–H Activation for the Synthesis of Divergent Heterocycles Bearing a Quaternary Carbon. *J. Org. Chem.* **2018**, *83*, 4650–4656. [CrossRef] [PubMed]

17. Allart-Simon, I.; Moniot, A.; Bisi, N.; Ponce-Vargas, M.; Audonnet, S.; Laronze-Cochard, M.; Sapi, J.; Hénon, E.; Velard, F.; Gérard, S. Pyridazinone derivatives as potential anti-inflammatory agents: Synthesis and biological evaluation as PDE4 inhibitors. *RSC Med. Chem.* **2021**, *12*, 584–592. [CrossRef]

18. Elmasry, G.F.; Aly, E.E.; Awadallah, F.M.; El-Moghazy, S.M. Design and synthesis of novel PARP-1 inhibitors based on pyridopyridazinone scaffold. *Bioorg. Chem.* **2019**, *17*, 655–666. [CrossRef]

19. Besada, P.; Viña, D.; Costas, T.; Costas-Lago, C.M.; Vila, N.; Torres-Terán, I.; Sturlese, M.; Moro, S.; Terán, C. Pyridazinones containing dithiocarbamoyl moieties as a new class of selective MAO-B inhibitors. *Bioorg. Chem.* **2021**, *115*, 105203. [CrossRef]

20. Li, B.; Wen, H.-M.; Wang, H.; Wu, H.; Yildirim, T.; Zhou, W.; Chen, B. Porous metal-organic frameworks with Lewis basic nitrogen sites for high-capacity methane storage. *Energy Environ. Sci.* **2015**, *8*, 2504–2511. [CrossRef]

21. Saquib, M.; Ansari, M.; Johnson, C.R.; Khatoon, S.; Hussain, M.K.; Coop, A. Recent advances in the targeting of human DNA ligase I as a potential new strategy for cancer treatment. *Eur. J. Med. Chem.* **2019**, *182*, 111657. [CrossRef] [PubMed]

22. Hamed, M.Y.; Aly, A.M.; Abdullah, N.H.; Ismail, M.F. Synthesis, Characterization and Antifungal Evaluation of Novel Pyridazin-3(2*H*)-One Derivatives. *Polycyc. Aromat. Compd.* **2022**. [CrossRef]

23. Gokce, M.; Utku, S.; Kupeli, E. Synthesis and analgesic and anti-inflammatory activities 6-substituted-3(2*H*)-pyridazinone-2-acetyl-2-(*p*-substituted/nonsubstituted benzal)hydrazone derivatives. *Eur. J. Med. Chem.* **2009**, *44*, 3760–3764. [CrossRef]

24. Rubat, C.; Coudert, P.; Tronche, P.; Bastide, J.; Bastide, P.; Privat, A.M. Synthesis and pharmacological evaluation of *N*-substituted 4, 6-diaryl-3-pyridazinones as analgesic, antiinflammatory and antipyretic agents. *Chem. Pharm. Bull.* **1989**, *37*, 2832–2835. [CrossRef]

25. Rathish, I.G.; Javed, K.; Bano, S.; Ahmad, S.; Alam, M.S.; Pillai, K.K. Synthesis and blood glucose lowering effect of novel pyridazinone substituted benzenesulfonylurea derivatives. *Eur. J. Med. Chem.* **2009**, *44*, 2673–2678. [CrossRef]

26. Abouzid, K.; Hakeem, M.A.; Khalil, O.; Maklad, Y. Pyridazinone derivatives: Design, synthesis, and In Vitro vasorelaxant activity. *Bioorg. Med. Chem.* **2008**, *16*, 382–389. [CrossRef]

27. Cao, S.; Qian, X.; Song, G.; Chai, B.; Jiang, Z. Synthesis and antifeedant activity of new oxadiazolyl 3(2*H*)-pyridazinones. *J. Agric. Food Chem.* **2003**, *51*, 152–155. [CrossRef]

28. Asif, M.; Singh, A.; Siddiqui, A.A. Effect of pyridazine compounds on cardiovascular system. *Med. Chem. Res.* **2012**, *21*, 3336–3346. [CrossRef]

29. Contreras, J.M.; Rival, Y.M.; Chayer, S.; Bourguignon, J.J.; Wermuth, C.G. Aminopyridazines as acetylcholinesterase inhibitors. *J. Med. Chem.* **1999**, *42*, 730–741. [CrossRef]

30. Grote, R.; Chen, Y.; Zeeck, A.; Chen, Z.X.; Zähner, H.; Mischnick-Lübbecke, P.; König, W.A. Metabolic products of microorganisms. 243. Pyridazomycin, a new antifungal antibiotic produced by Streptomyces violaceoniger. *J. Antibiot.* **1988**, *41*, 595–601. [CrossRef]

31. Horkel, E. Metalation of Pyridazine, Cinnoline, and Phthalazine. *Top Heterocycl. Chem.* **2013**, *31*, 223–268.

32. Schmidt, E.W. One Hundred Years of Hydrazine Chemistry. In Proceedings of the 3rd Conference on Environmental Chemistry of Hydrazine Fuels, Panama City Beach, FL, USA, 17 September 1988; pp. 4–16.

33. Moliner, A.M.; Street, J.J. Decomposition of Hydrazine in Aqueous Solutions. *J. Environ. Qual.* **1989**, *18*, 483–487. [CrossRef]

34. Wagnerová, D.M.; Schewertnerová, E.; Vepřek-Šiška, J. Autoxidation of hydrazine catalyzed by tetrasulphophthalocyanines. *Collect. Czech Chem. Commun.* **1973**, *38*, 756–764. [CrossRef]

35. Helal, A.; Qamaruddin, M.; Aziz, M.A.; Shaikh, M.N.; Yamani, Z.H. MB-UiO-66-NH2 metal-organic framework as chromogenic and fluorogenic sensor for hydrazine hydrate in aqueous solution. *ChemistrySelect* **2017**, *2*, 7630–7636. [CrossRef]

36. Sahin, T.; Vairaprakash, P.; Borbas, K.E.; Balasubramanian, T.; Lindsey, J.S. Hydrophilic bioconjugatable trans-AB-porphyrins and peptide conjugates. *J. Porphyr. Phthalocyanines* **2015**, *19*, 663–678. [CrossRef]

37. Hong, A.P.; Chen, T.-C. Catalyzed autoxidation of hydrazine by cobalt(II) 4,4′,4″,4‴-tetrasulfophthalocyanine. *Environ. Sci. Technol.* **1993**, *27*, 2404–2411. [CrossRef]

38. Hassan, H. Unanticipated Heterocyclization from Reaction of Hydrazine Hydrate and/or Hydrazine Dihydrochloride with 1-Ethyl-4-hydroxyquinolin-2(1*H*)-one. *J. Heterocycl. Chem.* **2019**, *56*, 646–650. [CrossRef]

39. Guanxing, Z.; Gang, Z. Access to a Phthalazine Derivative Through an Angular *cis*-Quinacridone. *J. Org. Chem.* **2021**, *86*, 1198–1203.

40. Le-Nhat-Thuy, G.; Thi, T.A.D.; Thi, Q.G.N.; Thi, P.H.; Nguyen, T.A.; Nguyen, H.T.; Thi, T.H.N.; Nguyen, H.S.; Nguyen, T. Synthesis and biological evaluation of novel benzo[*a*]pyridazino[3,4-*c*]phenazine derivatives. *Biorgan. Med. Chem. Lett.* **2021**, *43*, 128054. [CrossRef]

41. Zhang, Y.; Sim, J.H.; MacMillan, S.N.; Lambert, T.H. Synthesis of 1,2-Dihydroquinolines *via* Hydrazine-Catalyzed Ring-Closing Carbonyl-Olefin Metathesis. *Org. Lett.* **2020**, *22*, 6026–6030. [CrossRef]

42. Aly, A.A.; Hassan, A.A.; Mohamed, A.H.; Osman, E.M.; Bräse, S.; Nieger, M.; Ibrahim, M.A.A.; Mostafa, S.M. Synthesis of 3,3′-methylenebis- (4-hydroxyquinolin-2(1*H*)-ones) of prospective anti-COVID-19. *Mol. Divers.* **2021**, *25*, 461–471. [CrossRef] [PubMed]

43. Abass, M. Chemistry of substituted quinolinones. Part II synthesis of novel 4-pyrazolylquinolinone derivatives. *Synth. Commun.* **2000**, *30*, 2735–2757. [CrossRef]

44. Ismail, M.; Abass, M.; Hassan, M. Chemistry of substituted quinolinones. Part VI. Synthesis and nucleophilic reactions of 4-chloro-8-methylquinolin-2(1*H*)-one and its thione analogue. *Molecules* **2000**, *5*, 1224–1239. [CrossRef]

45. Ismail, M.; Abdel-Megid, M.; Hassan, M. Some reactions of 2-and 4-substituted 8-methylquinolin-2(1*H*)-ones and their thioanalogues. *Chem. Papers Slovak Acad. Sci.* **2004**, *58*, 117–125.

46. Aly, A.A.; Sayed, S.M.; Abdelhafez, E.M.N.; Abdelhafez, S.M.N.; Abdelzaher, W.Y.; Raslan, M.A.; Ahmed, A.E.; Thabet, K.; El-Reedy, A.A.M.; Brown, A.B.; et al. New quinoline-2-one/pyrazole derivatives; design, synthesis, molecular docking, antiapoptotic evaluation, and caspase-3 inhibition assay. *Bioorg. Chem.* **2020**, *94*, 103348. [CrossRef]

47. Hofmann, J.; Jasch, H.; Heinrich, M.R. Oxidative Radical arylation of anilines with arylhydrazines and dioxygen from Air. *J. Org. Chem.* **2014**, *79*, 2314–2320. [CrossRef]

48. Liu, W.; Twilton, J.; Wei, B.; Lee, M.; Hopkins, M.N.; Bacsa, J.; Stahl, S.S.; Davies, H.M.L. Copper-catalyzed oxidation of hydrazones to diazo compounds using oxygen as the terminal oxidant. *ACS Catal.* **2021**, *11*, 2676–2683. [CrossRef]

49. Bader, R.F.W. Atoms in Molecules. *Acc. Chem. Res.* **1985**, *18*, 9–15. [CrossRef]

50. Johnson, E.R.; Keinan, S.; Mori-Sanchez, P.; Contreras-Garcia, J.; Cohen, A.J.; Yang, W. Revealing noncovalent interactions. *J. Am. Chem. Soc.* **2010**, *132*, 6498–6506. [CrossRef]

51. Sheldrick, G.M. SHELXT—Integrated space-group and crystal-structure determination. *Acta Crystallogr.* **2015**, *71A*, 3–8. [CrossRef]

52. Parson, S.; Flack, H.D.; Wagner, T. Use of intensity quotients and differences in absolute structure refinement. *Acta Crystallogr.* **2013**, *69B*, 249–259. [CrossRef] [PubMed]

53. Becke, A.D. Density-functional exchange-energy approximation with correct asymptotic behavior. *Phys. Rev. A* **1988**, *38*, 3098–3100. [CrossRef] [PubMed]

54. Lee, C.; Yang, W.; Parr, R.G. Development of the Colle-Salvetti correlation-energy formula into a functional of the electron density. *Phys. Rev. B* **1988**, *37*, 785–789. [CrossRef] [PubMed]

55. Krishnan, R.; Binkley, J.S.; Seeger, R.; Pople, J.A. Self-consistent molecular orbital methods. XX. A basis set for correlated wave functions. *J. Chem. Phys.* **1980**, *72*, 650–654. [CrossRef]

56. Lu, T.; Chen, F.; Multiwfn, F. A multifunctional wavefunction analyzer. *J. Comput. Chem.* **2012**, *33*, 580–592. [CrossRef]

57. Humphrey, W.; Dalke, A.; Schulten, K. VMD: Visual molecular dynamics. *J. Mol. Graph.* **1996**, *14*, 33–38. [CrossRef]

58. Frisch, M.J.; Trucks, G.W.; Schlegel, H.B.; Scuseria, G.E.; Robb, M.A.; Cheeseman, J.R.; Scalmani, G.; Barone, V.; Mennucci, B.; Petersson, G.A.; et al. *Gaussian 09, Revision E.01*; Gaussian, Inc.: Wallingford, CT, USA, 2009.